Desorption of Lead Ions from Used Sodium Alginate-Hydroxypropyl Cellulose Adsorbent Beads

Rodel D. Guerrero[1*], Imee Kassandra E. Cacho[1], Dan Michael A. Asequia[1],

Joshua Emmanuel L. Hugo[1]

[1] Department of Chemical Engineering and Technology, College of Engineering and Technology, MSU-Iligan Institute of Technology, Iligan City, Philippines
*Corresponding Author: rodel.guerrero@g.msuiit.edu.ph

Abstract. Efficient removal of adsorbed lead ions from the sodium alginate-hydroxypropyl cellulose beads was necessary to guarantee their long-term use for repeated adsorption-desorption cycles. In this study, the desorption characteristics of previously adsorbed lead ions on sodium alginate-hydroxypropyl (SA-HPC) cellulose adsorbent beads were tested using various eluents such as sulfuric acid and ethylenediaminetetraacetic acid (EDTA). SA-HPC adsorption beads were produced using 3:1 ratio of sodium alginate to hydroxypropyl cellulose via ionotropic gelation. Generally, using H_2SO_4 as eluent maintained an exceptional adsorption efficiency throughout in each cycle, but showed a weak desorption efficiency performance. The desorption efficiency using 0.1M EDTA, on the other hand, was found to be the most effective but resulted to the beads disintegration after the first cycle.

Index Terms: sodium alginate, hydroxypropyl cellulose, adsorption, desorption, eluent, lead

I. INTRODUCTION

Industries such as electroplating, metal finishing, textile, storage batteries, mining, ceramic and glass discharge heavy metals along with its wastes. These metal contaminants of wastewater are mainly mercury (Hg), cadmium (Cd), chromium (Cr), arsenic (As) and lead (Pb). Contamination of various water resources by these heavy metals is a concern requiring urgent relevant action because of their detrimental effect on human, animal and plants [1]. Posing serious environmental problems worldwide, much attention has been given to the methods for their removal from industrial wastewaters. Typical procedures used for removing metal ions include chemical precipitation, ion exchange, membrane separation, reverse osmosis, evaporation and electrolysis, lime coagulation and solvent extraction. However, these techniques are somehow disadvantageous due to incomplete removal of metal ions, high reagent requirements, generation of toxic sludge and other added wastes products that require treatment and disposal [2].

The pursuit for advanced and unconventional treatment techniques has focused attention on the use of biological materials such as algae, fungi, yeast and bacteria for the removal and recovery technologies and is continually advancing during recent years because of the better performance and low cost of these biological materials [3,4,5]. One such strategy is biosorption which is binding of metal ions with metal binding proteins present on the cell wall. Not only is it exhibited by living organisms, but also residuals of dead bodies of microorganisms shows biosorbent properties like agricultural wastes including husk, seeds, peels and stalks of different crops [6]. Technologies on biosorption based on the use of dead biomass is preferable and expedient because its less toxic, no need of nutrient supply and is efficient in the recovery of bound metal species provided an appropriate desorption method [7]. Wilde and Benemann in 1993 states the significance of biopolymers in relevance to removal of heavy metals apart from its non-toxic composition, selectivity, inexpensive and thus highly competitive with ion exchange resins and activated carbon.

Knowing biopolymer as an essential tool for biosorption, choice of what kind of biopolymer is significant in the sorption process especially when utilized for successive sorption-desorption process [8]. Various biopolymers such as alginate, gluteraldehyde, agarose, cellulose – acetate derived from microorganisms and plants are known to bind metal ions strongly and could be used for heavy metal adsorption [2]. A previous study conducted by Alarde et. al [9] in 2019, focused on the adsorption process of removing lead ions from aqueous solutions using synthetic hydrogel-forming polymer based on Hydroxypropyl cellulose (HPC) and sodium alginate (SA) and determined the adsorption capacity and percentage of the adsorbents. The feasibility of

adsorption behavior of the SA-HPC beads were investigated with three varying ratios of 50:50, 75:25 ad 100:0. The results then declared that the 75:25 or the 3:1 ratio has the highest adsorption capacity of 47.72 mg/g and an adsorption percentage of 94.45% after three (3) hours of contact time. Furthermore, having found out that the adsorption follows a pseudo-second order kinetics, the sole rate-limiting step is only the interparticle diffusion. Finally, it was shown that the diffusivity is directly proportional to the SA-HPC ratio.

However, previous studies for that matter haven't made any consideration with respect on the capacity of reusability in multiple adsorptions – desorption cycles. As a result, this study will investigate the desorption profile and reusability of sodium alginate and hydroxypropyl cellulose adsorbent beads used in the removal of Pb(II) in aqueous solution.

II. MATERIALS AND METHODS

2.1 Materials

Chemicals used in the study were Sodium Alginate (SA) from Sterling Galeon Corporation, Philippines; Hydroxypropyl Cellulose (HPC) powder from FreyaLab, DCI of Bulgaria; Calcium Chloride powder from Sigma-Aldrich Pte. Ltd., from Singapore with 99.99% trace metals basis; and Lead Chloride powder with $\geq$99% trace metals basis from Uni-Chem Chemical Reagents, Philippines. All other reagents were of analytical grade and used as received.

2.2 Methods

2.2.1 Preparation of Beads

Solution of two (2) weight percent of the material was prepared using the 3:1 ratio of sodium alginate to hydroxypropyl cellulose. It was dissolved in distilled water and the resulting solution was then stirred at room temperature until solution was homogenized.

The blended sodium alginate and hydroxypropyl cellulose solution was extruded through a syringe in the form of droplets then cured into a five (5) weight percent crosslinking solution ($CaCl_2$) for 15 minutes to form the beads. Afterwards, the beads were dried in the oven at 45℃ for at least five hours.

2.2.2 Bead Size Measurement

Different diameters of beads were obtained and were calculated according to their mean diameter. Mean diameter was used as the initial diameter size of the bead upon getting the swelling ratio of the bead after the simulation using the following equation:

$$mean\ diameter = \frac{Sum\ of\ the\ bead's\ diameter}{Number\ of\ beads} \qquad (1)$$

2.2.3 Treatment

2.2.3.1 Batch Adsorption

A 0.10xx gram of SA-HPC beads was contained in a volumetric flask. Aliquot of 25 ml from the 200 ppm lead chloride solution was mixed with the beads in the volumetric flask. The mixture was stirred for 180 minutes at a rate 150 rpm. It was then filtered then washed with distilled water to remove surface metal and is dried at a temperature of 45℃ for 5 hours. The diameter of the beads (before and after adsorption) were also measured.

2.2.3.2 Contact Time for Desorption

SA-HPC beads used in the adsorption of lead metal ions were subjected to desorption using H_2SO_4 and EDTA solutions (all in 0.1 M concentration). Twenty-five milliliters of each eluent was added in a volumetric flask with the batch of 0.10xx g of beads used from the previous adsorption. Contact time for desorption were then recorded for 60 minutes, 120 minutes and 180 minutes at a rate of 150 rpm. Beads after desorption were filtered and washed with distilled water to remove surface metal and dried at temperature of 45℃ for 5 hours. Measuring of beads' diameter were also done.

2.2.3.3 Recycling of Beads

After drying, another cycle of adsorption-desorption process was done according to the methods aforementioned.

2.2.4 Theoretical Relations

2.2.4.1 Desorption Efficiency

The desorption efficiency was calculated from the amount of metal ions adsorbed on the adsorbent and the final metal ion concentration in the adsorption medium using the following equation:

$$Desorption\ efficiency = \frac{amount\ of\ lead\ ions\ desorbed}{amount\ of\ lead\ ions\ adsorbed} \times 100 \qquad (2)$$

2.2.4.2 Degree of Reusability

A simulation for the adsorption-desorption process of different eluents of corresponding time for three cycles were done. A batch of beads underwent adsorption for 180 min and then desorption for 60 min. After being washed and dried, the process was then repeated for the second and third cycle. The other batches of beads were treated the same until completion.
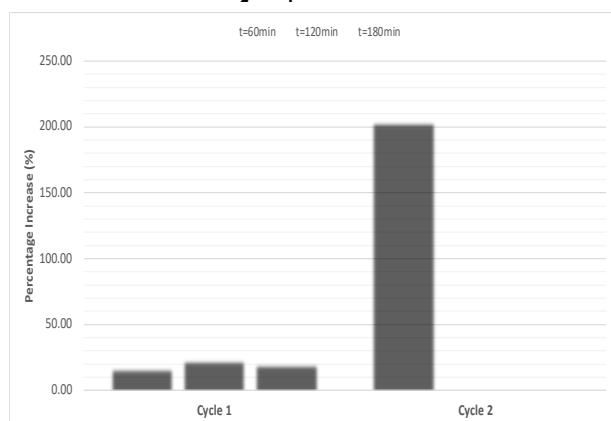
III. RESULTS AND DISCUSSION

3.1. Adsorbent Size Analysis

The diameters of the beads were measured before and after the adsorption-desorption process. The results can be summarized in the figures below.
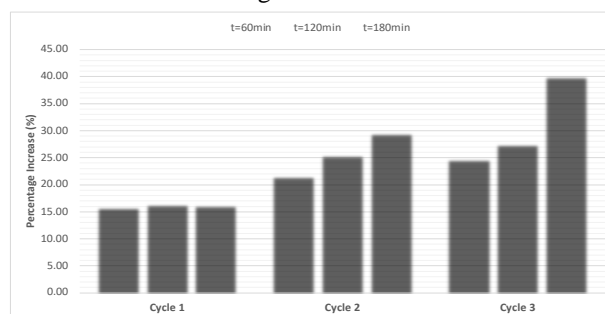
Figure 1. Percent increase in diameter of SA-HPC beads for three adsorption-desorption cycles using H$_2$SO$_4$ as eluent.


Figure 2. Percent increase in diameter of SA-HPC beads for two adsorption-desorption cycles using EDTA as eluent.

During the first cycle in adsorption, the data above (Figure 1) shows a negligible difference in terms of percent increase of the bead diameter before and after the adsorption process. This is expected to happen because during adsorption, the beads were treated under the same conditions. It is in the second and third cycles that it can be seen in the graph an increasing trend of swelling percentage. This is because of the effect of being immersed in H$_2$SO$_4$ acid solution during desorption process. The molecule H$_2$SO$_4$ being a strong acid tend to form a hydrogen bond with the crosslinked SA-HPC beads which then loosen the bonds and rigidity of the beads. The longer the beads are immersed H$_2$SO$_4$ in the desorption process, the more it swells during adsorption process.

Meanwhile, the second cycle in adsorption-desorption using EDTA as eluent in figure 2 shows a drastic change in beads diameter. There is an increase of more than 200% of the bead's diameter before the adsorption process and reaching the wet beads diameter after the crosslinking preparation of beads before drying it in the oven. Additionally, after adsorption for time 120 minutes, it is then impossible to measure the beads diameter because it is already feeble and out of shape.
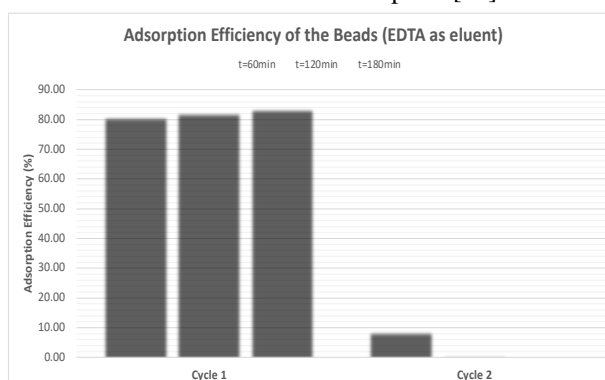
3.2. Adsorption Efficiency

The adsorption capacity and efficiency of the beads at varying time were calculated using the data based on the amount of lead concentration left in the solution after the adsorption process. The results can be summarized as shown these figures.
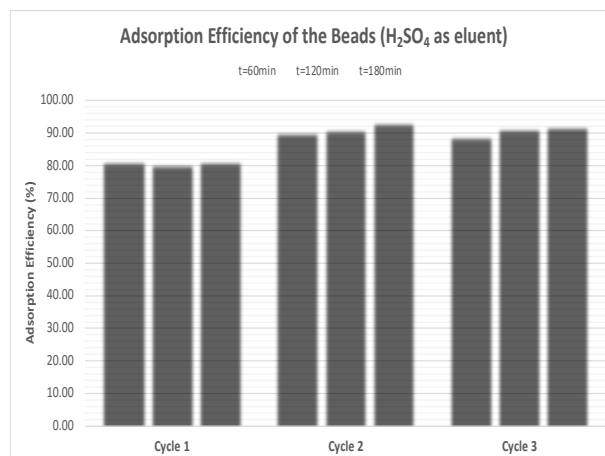
Figure 3. Adsorption efficiencies of SA-HPC beads (H$_2$SO$_4$ as eluent)

This data (figure 3) shows the adsorption efficiency of the beads using H$_2$SO$_4$ as eluent, respectively. There is about 10% increase of the values from cycle 1 to cycle 2 and a slight difference from cycle 2 to cycle 3. One possible explanation for this is that when the beads are immersed in H$_2$SO$_4$, the hydrogen bonding competes the ionic crosslinking of the beads that leads to disintegration of the beads thus increasing the surface area of the beads available for adsorption [10].
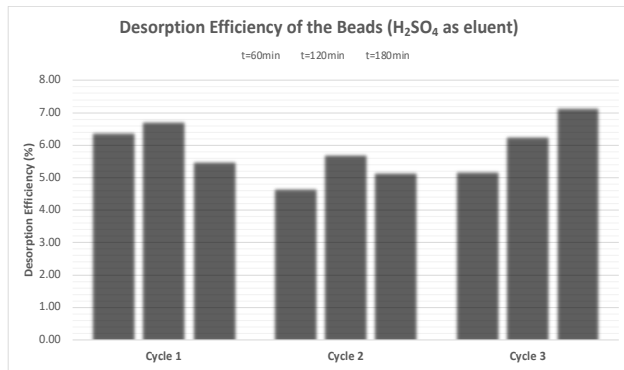

Figure 4. Adsorption efficiencies of SA-HPC beads (EDTA as eluent)

On the other hand, this figure 4 depicts the adsorption efficiency of the beads using EDTA as eluent. While the adsorbents projected a great adsorption efficiency on its first use, there is a drastic decrease of the adsorption capacity and efficiency of the beads when it was reused. This is mainly due to the fact that when the beads were immersed in EDTA, there happens a reversible crosslinking that reverted the beads back to its gel-like form, barely holding to its spherical shape. Hence, it was not suitable to undergo more cycles [11].
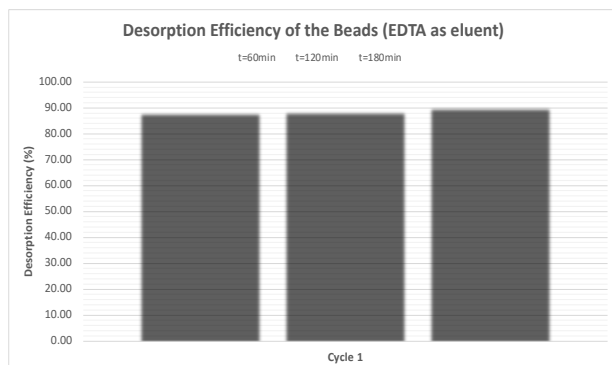
3.3. Desorption Efficiency

For the desorption efficiency data, this graph shows the desorption efficiency using H$_2$SO$_4$ solution as eluent. The graph shown technically does not follow a uniform trend of desorption efficiency at different contact time within each cycle and at different cycles. However, it definitely presents a weak desorption efficiency of using sulfuric acid as eluent ranging from around 4-8 % only.

Figure 5. Desorption efficiencies of SA-HPC beads (H$_2$SO$_4$ as eluent)

Sulfuric acid (H$_2$SO$_4$) is a strong mineral acid which means that it dissociates in water completely as either a hydrogen sulfate ion or a sulfate ion, and is capable to form hydrogen bonding with the alginate. The H$_2$SO$_4$ can then act as a monodentate or bidentate ligand but is expected to be a weak field ligand because the available atom to bind is oxygen which is one of the most electronegative atoms.

Additionally, for EDTA as eluent, this result depicts that there is a slight increasing desorption efficiency with increasing contact time. This is because EDTA being a strong field ligand maximizes its activity in desorbing metal ions as contact time increases. However, it was only used for one desorption cycle as it reverted back the beads into gel forms.


**Figure 6. Desorption efficiencies of SA-HPC beads (EDTA as eluent)**

During this desorption process, the ionic crosslinking is being altered with hydrogen bonding and chelation of metal ions either Ca^{2+} or Pb^{2+} by H$_2$SO$_4$. This occurrence validates the observed disintegration of the beads when immersed in H$_2$SO$_4$. The H$_2$SO$_4$ as eluent competes the ionic crosslinking of the beads. As a result, the structure of the beads is altered, it creates pores on the beads, and the beads are then broken into small pieces. This phenomenon provides more binding site for chemisorption of the beads during adsorption. According to Petrovic & Simonic [12] in 2016, that chemisorption follows three steps. First is where the lead ions are bonded to the binding sites containing functional groups like the carboxyl group in the alginate. Second is where diffusion of lead ions into pores of adsorbent and the last step is the diffusion of lead ions into the internal surface of the beads.

3.4. Adsorption-Desorption Profile

From the data gathered, the adsorption-desorption profile of the SA-HPC beads for different eluents are shown in Figure 7.
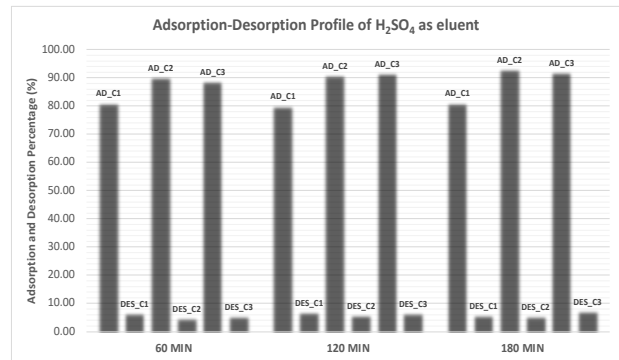
(a)
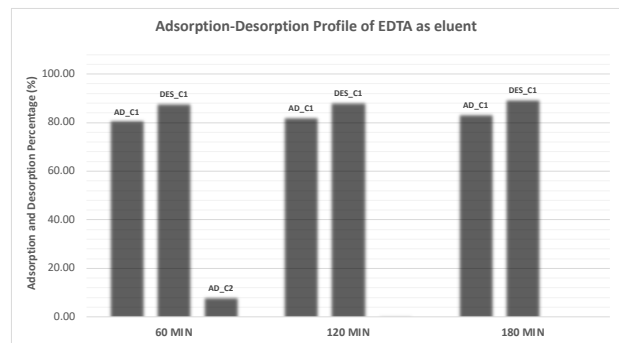
(b)

Figure 7. Adsorption-desorption profiles of SA-HPC adsorbent beads using (a) H$_2$SO$_4$ and (b) EDTA as eluent with respect to desorption's contact time.

An identical trend is noticeable in each eluent throughout the cycle. Additionally, it can be verified in the figures above that adsorption-desorption efficiency is not significantly different at various time. However, the results exhibit that using H$_2$SO$_4$ as eluent maintains an exceptional adsorption efficiency throughout in each cycle yet shows a weak desorption efficiency performance. On the other hand, when EDTA is being used as eluent, the desorption efficiency is way greater than using H$_2$SO$_4$ as eluent. Nevertheless, using H$_2$SO$_4$ as eluent renders to more number of cycle which means a greater in degree of reusability than using EDTA as eluent.

IV.   CONCLUSION

In conclusion, the study was successful in establishing desorption profiles for the adsorbent beads used in a simulation of a lead ion contaminated water using sodium alginate and hydroxypropyl adsorbent beads. Beads subjected to H$_2$SO$_4$ as eluent generally maintains an exceptional adsorption performance. For EDTA as eluent, due to the reversal effect, its adsorption capacity and efficiency drastically decreases from cycle 1 to cycle 2 which also means that it is inappropriate to proceed more cycles.

Furthermore, For H$_2$SO$_4$ as eluent, the desorption efficiency at different cycle is significant, but the

desorption contact time is not. Average desorption efficiency recorded is around 5.86%. For EDTA as eluent, the desorption efficiency showed average of 88.58%. However, it is only good for one cycle as it tends to disintegrate the beads themselves. using H_2SO_4 as eluent renders to more number of cycle which means a greater in degree of reusability than using EDTA as eluent.

REFERENCES

1. Neethu, T. M., Dubey, P. K., & Kaswala, A. R. (2018). Prospects and Applications of Hydrogel Technology in Agriculture. International Journal of Current Microbiology and Applied Sciences, 7(5), 3155–3162. https://doi.org/10.20546/ijcmas.2018.705.369

2. Akalin, G. O., & Pulat, M. (2018). Preparation and Characterization of Nanoporous Sodium Carboxymethyl Cellulose Hydrogel Beads. Journal of Nanomaterials, 2018, 1–12. https://doi.org/10.1155/2018/9676949

3. Rees, D. A. (1969). Structure, Conformation, and Mechanism in the Formation of Polysaccharide Gels and Networks. In Advances in Carbohydrate Chemistry and Biochemistry (pp. 267–332). https://doi.org/10.1016/s0065-2318(08)60352-2

4. Clark, A. H., & Ross-Murphy, S. B. (n.d.). Structural and mechanical properties of biopolymer gels. In Biopolymers (pp. 57–192). https://doi.org/10.1007/bfb0023332

5. Hilmi, B., Hamid, Z. A. A., Akil, H. M., & Yahaya, B. H. (2016). The Characteristics of the Smart Polymers Temperature or pH-responsive Hydrogel. Procedia Chemistry, 19, 406–409. https://doi.org/10.1016/j.proche.2016.03.031

6. Garduque, R.G., Gococo, B.J., & Yu, C.A. (2019). Synthesis and characterization of sodium carboxylmethyl cellulose/hydroxypropyl cellulose/sodium alginate hydrogel for agricultural water storage and controlled nutrient release. Bachelor of Science in Chemical Engineering: University of the Philippines Diliman.

7. Ayatullah Hosne Asif, A. K. M., Rahman, M., Sarker, P., Hasan, M. Z., & Paul, D. (2019). Hydrogel Fibre: Future Material of Interest for Biomedical Applications. Journal of Textile Science and Technology, 5(4), 92–107. https://doi.org/10.4236/jtst.2019.54009

8. Arifuzzaman Md., Wu Z.L., Takahashi R. Kurokawa T. Nakajima T. & Gong J.P. (2013). Geometric and Edge Effects on Swelling-induced Ordered Structure Formation in Polyelectrolyte Hydrogels. Macromolecules 2013, 46,22, 9083-9090. https://doi.org/10.1021/ma401773w

9. Reddy, S. G., Pandit, A. S., & Thakur, A. (2016). Effects of Crosslink Agents on Sodium Alginate and Lignosulphonic Acid Blends. Polymer Korea, 40(1), 63. https://doi.org/10.7317/pk.2016.40.1.63

10. Reddy, S. G. & Akanksha, S. P. (2011). Swelling Behavior of Calcium–Ions Crosslinked Bipolymeric Sodium Alginate–Lignosulphonic Acid Blends. International Journal of Polymeric Materials, 60(14), 1123–1129. https://doi.org/10.1080/00914037.2011.553855

11. Ganji, F., Vasheghani, F. S., & Vasheghani, F. E. (2010). Theoretical description of hydrogel swelling: a review. Iranian Polymer Journal, 19(5), 375-398.

12. Ritger, P. L., & Peppas, N. A. (1987). A simple equation for description of solute release I. Fickian and non-fickian release from non-swellable devices in the form of slabs, spheres, cylinders or discs. Journal of Controlled Release, 5(1), 23–36. https://doi.org/10.1016/0168-3659(87)90034-4

13. Abdel-Raouf, M. E., El-Saeed, S. M., Zaki, E. G., & Al-Sabagh, A. M. (2018). Green chemistry approach for preparation of hydrogels for agriculture applications through modification of natural polymers and investigating their swelling properties. Egyptian Journal of Petroleum, 27(4), 1345–1355. https://doi.org/10.1016/j.ejpe.2018.09.002

14. An, D., Yang, L., Liu, B., Wang, T.-J., & Kan, C. (2017). Diffusion Performance of Fertilizer Nutrient through Polymer Latex Film. Journal of Agricultural and Food Chemistry, 65(50), 10868–10874. doi:10.1021/acs.jafc.7b04225

15. Anton Paar GmbH (2020). Anton Paar Wiki. Viscosity of Water – viscosity table and viscosity chart. Retrieved from https://wiki.anton-paar.com/en/water/ on 1 June 2020.

16. Rizwan, M., Yahya, R., Hassan, A., Yar, M., Azzahari, A., Selvanathan, V., Sonsudin F. & Abouloula C. (2017). pH Sensitive Hydrogels in Drug Delivery: Brief History, Properties, Swelling, and Release Mechanism, Material Selection and Applications. Polymers, 9(12), 137. https://doi.org/10.3390/polym9040137

17. Catoria M. Fusaro L. Fancesco D. Ramella M. & Boccafoschi F. (2019) Overview of natural hydrogels for regenerative medicine applications. Journal of Materials Science. Materials in Medicine 30(10): 115. https://www.ncbi.nlm.nih.gov/pmc/articles/PMC6787111/